A POPULATION BALANCE MODEL OF CELL CYCLE-SPECIFIC TUMOR GROWTH

Jeffry A. Florian, Jr. [*] **Robert S. Parker** [*,1]

[*] *Department of Chemical and Petroleum Engineering*
University of Pittsburgh, Pittsburgh, PA USA

Abstract: Chemotherapeutics are often treated as having a lumped tumor effect, however, the growth state and exposure for individual cancer cells ultimately determines the response of the tumor to treatment. A multi-staged, age structured cell population balance equation (PBE) capable of cell-cycle tracking was formulated to account for this limitation. The method of orthogonal collocation on finite elements was used to decompose the original partial differential and algebraic equation formulation into a system of nonlinear ODEs with a renewal algebraic equation for age zero cells. The model was then adapted to include growth inhibitory effects and drug induced apoptosis specific to the S-phase for the testing of two theoretical drugs in adjuvant therapy. Simulations evaluated the delivery of apoptotic drug alone, or both drugs in combination. Increases in overall tumor reduction resulted from the adjuvant therapy, typical of results observed experimentally. Additional refinement is necessary regarding transition, division, and apoptotic intensity function construction prior to clinical application, but this model represents a feasible structure for describing distributed tumor progression with incorporated drug effect.

Keywords: medical systems, nonlinear dynamical modelling

1. INTRODUCTION

Cancer, a disease characterized by an imbalance between cell growth and apoptosis, is the second leading cause of death in the United States, responsible for a quarter of health related fatalities each year (The American Cancer Society, 2004). In addition, an expected 1.4 million new cancer cases are expected during 2004, not including 1 million new cases of carcinoma *in situ* or skin cancer (The American Cancer Society, 2004). As such, any improvements in cancer treatment, through drug discovery, diagnostic capabilities, or dosing regimens, could have significant impacts on economic cost and cancer prognosis. Dosing regimen development, accomplished using past experience, preliminary pharmacological data, and trial and error methods, can also be posed in a model-based framework. The goal of model-based cancer treatment algorithms is to minimize some objective, such as final tumor volume or patient toxicity, over a fixed treatment duration. The underlying tumor model upon which the algorithm is based, however, will ultimately limit the theoretically achievable level of algorithm performance (Morari and Zafiriou, 1989).

Traditional models for describing tumor growth include lumped exponential or Gompertz models (Norton, 1988; Martin and Teo, 1994; Harrold *et al.*, 2003), where the latter displays saturating growth as a function of increasing tumor volume. Though both models accurately describe bulk tumor progression over fixed time periods, modeled drug effects are incorporated as affecting the entire population equally. While this would be true for a chemotherapeutic capable of inducing apoptosis independent of a cell state, the majority of cancer drugs display increased lethality during particular phases of cell growth (so-called cell-cycle specific chemotherapeutics). Indeed,

[1] To whom correspondence should be addressed: rparker@pitt.edu; +1-412-624-7364; 1249 Benedum Hall, Pittsburgh, PA 15261 USA

failure to incorporate cell cycle phases within a model can lead to significant controller performance loss depending on the cycle-specificity of the chemotherapeutic (Florian Jr. *et al.*, 2004).

Cell-cycle models, displaying either exponential or saturating growth (Panetta and Adam, 1995; Florian Jr. *et al.*, 2003), divide a lumped tumor approximation into multiple lumped cell phases, allowing for drug-effect inclusion in the appropriate phase of growth. Such lumped models treat all cells within a given cell phase as having equivalent drug exposure. Apoptotic response is often modeled as a bilinear combination of drug concentration and susceptible population size, premultiplied by a rate constant corresponding to drug activity and tumor sensitivity. However, a tumor is a heterogeneous population of cells with drug exposures dependent on the surrounding vasculature for systemically delivered drugs (Brown and Giaccia, 1998). Furthermore, drug-induced apoptosis may be a function of period of exposure, point of exposure within a cell phase, or additional intracellular states. Even radiation therapy displays an apoptotic effect dually dependent on cell phase (increased susceptibility during G_2/M phase) and cellular oxygen concentration (increased probability of free radical formation) (Coleman and Mitchell, 2001).

The only models in the literature which account for distributed properties in a cell population are the aptly named, cell population balance models. This mathematical formulation allows for distributed internal properties (e.g. mass, age, DNA, protein) among a population, including the partitioning of intracellular compounds following cell division. In addition, this structure can account for intra-phase tumor population variability, such as distributed growth rates and different functional formulations of apoptotic effect. While the original cell population description dates back to Fredrickson, Ramkrishna, and Tsuchiya (1967), these models have recently seen increased use in bio-processes (Ramkrishna, 2000; Zhu *et al.*, 2000; Daoutidis and Henson, 2002; Mantzaris *et al.*, 2002; Zamamiri *et al.*, 2002). Historically, the primary limitations on cell PBE implementation were the numerical complexity of the partial integro-differential equations resulting from model development and difficulty in determining partition and transition functions and single-cell growth rates. However, with the development of numerical algorithms capable of accurately approximating PBE solutions, along with experimental advances for evaluating cellular properties, PBEs represent a viable option for modeling intracellular states as distributed properties among a cell population.

2. MODEL DEVELOPMENT

There are two common formulations for the cell population balance models which differ by internal

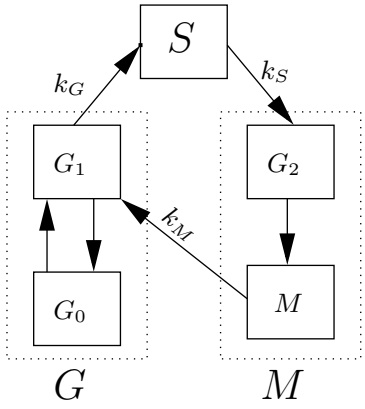

Fig. 1. The five phases of the cell-cycle: G_0 (senescence), G_1 (growth), S (DNA replication), G_2 (mitotic preparation), M (mitosis). Experimental methods (fluorescent DNA labeling and flow cytometry) limit resolution of G_0 from G_1 (lumped as G) and G_2 from M (lumped in M).

coordinates. Models with intracellular properties that obey mass conservation are referred to as mass structured while age distribution models differentiate between cells of different ages within the system. Both model structures have been explored for bioreactor applications, specifically the modeling of yeast cultures for single-phase, single-variable (Ramkrishna, 2000) and multi-phase, single variable (Zhu *et al.*, 2000; Daoutidis and Henson, 2002; Mantzaris *et al.*, 2002; Zamamiri *et al.*, 2002) cases with environmental coupling to the extracellular environment.

For implementation based on an adapted three cell cycle model (Figure 1), a mass structured model would require information on phase transition rates, a partitioning function for allocating cell properties following cell division, and single-cell growth rates for each phase. A model based solely on mass as the intrinsic variable would be unable to account for cell distributions within a senescent phase (G_0) where mass accumulation is theoretically zero (Kastan and Skapek, 2001). While senescent phase modeling was not included in the present analysis, selecting an alternative model structure would maintain model versatility for future work without requiring the inclusion of additional internal variables (and additional partitioning and accumulation rates). Finally, a mass structured cell-cycle model does not allow for explicit period of drug exposure calculation.

Age based models offer several advantages over mass structured cell population models even though age is not an available measure from a cell population. First, single cell rates of change for age correspond to unity, eliminating the need for experimentally determining three growth equations. Second, mass structured models formulate as partial integro-differential equations, a function of property partitioning following

cell division, while age structured models result in simpler partial differential equations with an integral boundary condition. This integral boundary condition results from the accumulation of newborn cells all of which possess an initial age of zero. Subsequently, calculation of a partition function is no longer required since age is not partitioned following cell division. Finally, tracking the internal property, age, allows for direct calculation of the period of drug exposure for any portion of the population. Drug-kill rates need not be constant throughout a cell phase, representative of complex interactions between a chemotherapeutic, intracellular targets, and the induction of apoptosis. For classes of problems where the dynamic effect of interest (tumor-kill) is period or point of exposure dependent, an age structured model is both less complex and more relevant.

3. CELL CYCLE TUMOR GROWTH PBE

The current model was adapted from the age structured yeast model developed by Zamamiri *et al.* (2002). For the three cell phases, G, S, and M, the cell phase population density is given by N_G, N_S, and N_M, respectively. The cell cycle PBE was constructed with cell-cycle specific drug effects in the S-phase, though the model can be adapted for cycle-specificity in any phase. As cycle-specific chemotherapeutics can inhibit progression through a cell cycle phase (*e.g.* cytarabine (Halicka *et al.*, 1997)) or directly induce apoptosis within a cycle (*e.g* camptothecin, irinotecan (Halicka *et al.*, 1997)), both effects were incorporated within the model structure. Here, drug dosing is modeled as a discrete input (*i.e.* ingesting a pill) which must be absorbed from the gut (Equations (4) and (6)) before reaching the plasma (Equations (5) and (7)). The complete PBE, with coupled drug effect formulation, is given by the following equations:

$$\frac{\partial N_G(a,t)}{\partial t}+\frac{\partial N_G(a,t)}{\partial a}=-\Gamma_G(a)N_G(a,t) \quad (1)$$

$$\frac{\partial N_S(a,t)}{\partial t}+\frac{\partial N_S(a,t)}{\partial a}=-\Gamma_S(a,D_1(t))N_S(a,t) - \Gamma_E(a,E_1(t))N_S(a,t) \quad (2)$$

$$\frac{\partial N_M(a,t)}{\partial t}+\frac{\partial N_M(a,t)}{\partial a}=-\Gamma_M(a)N_M(a,t) \quad (3)$$

$$\frac{dE_0(t)}{dt}=-k_{E0}E_0(t)+u_E(t) \quad (4)$$

$$\frac{dE_1(t)}{dt}=-k_{E1}E_1(t)+k_{E0}E_0(t) \quad (5)$$

$$\frac{dD_0(t)}{dt}=-k_{D0}D_0(t)+u_D(t) \quad (6)$$

$$\frac{dD_1(t)}{dt}=-k_{D1}D_1(t)+k_{D0}D_0(t) \quad (7)$$

Here, a is the period of time a cell has resided within a given phase. $D_1(t)$ is the concentration of the drug inhibiting transition from S to M phase, $E_1(t)$ is the concentration of the apoptosis-inducing drug, $E_0(t)$ and $D_0(t)$ represent drug concentrations within the gut and $u_D(t)$ and $u_E(t)$ are doses of the delaying and eliminating drugs, respectively. The transition functions out of cell phase G and M are $\Gamma_G(a)$ and $\Gamma_M(a)$, respectively, and $\Gamma_S(a,D_1(t))$ is the S-phase transition rate which is both a function of age and the concentration of the transition inhibiting drug. Finally, $\Gamma_E(a,E_1(t))$ is the S-phase-specific apoptotic effect which is a function of age and the concentration of the eliminating drug. Equation (2) reflects drug dependent effects on tumor-kill and tumor growth.

The G-phase transition function, $\Gamma_G(a)$, and M-phase division function $\Gamma_M(a)$, were assumed to have the following forms:

$$\Gamma_i(a)=\begin{cases} 0 & a\le a_{c_i} \\ \beta_i\frac{a-a_{c_i}}{(m_i-1)a_{c_i}}, & a_{c_i}\le a\le m_i a_{c_i} \\ \beta_i & m_i a_{c_i}\le a \end{cases} \quad (8)$$

Here, a_{c_i} is the critical age during cell phase i (where i = G or M) representing the minimal age necessary for phase transition or cell division onset. β_i represents the maximum transition rate for the cell phase and m_i defines the sharpness of the transition function subject to the additional constraint, $m_i > 1$, to ensure positive growth rates.

The S-phase transition rate, $\Gamma_S(a,D_1(t))$ has the modified form:

$$\Gamma_S(a,D_1(t)) = \begin{cases} 0 & a\le a_{nc_S} \\ \beta_S\frac{a-a_{nc_S}}{(m_S-1)a_{nc_S}}, & a_{nc_S}\le a\le m_S a_{nc_S} \\ \beta_S & m_S a_{nc_S}\le a \end{cases} \quad (9)$$

$$a_{nc_S}(a_{c_S},D_1(t))=a_{c_S}(1+\frac{K_M D_1(t)}{D_1(t)+m_D}) \quad (10)$$

The new critical age allowing for S-phase transition, a_{nc_S}, is a function of drug-free critical age, a_{c_S}, and the transition inhibiting drug concentration, $D_1(t)$. The parameter m_D affects the sharpness of the transition function with respect to drug concentration such that higher values of m_D reflect a more gradual increase in transition function value. β_S and m_S are equivalent to their G- and M-phase counterparts. The S-phase transition function is shown graphically in Figure 2. The G- and M-phase functions are identical to the $D_1(t)=0$ case. The S-phase specific apoptosis function was set to $\Gamma_E(a,E_1(t))=k_A a E_1(t)$ where k_A is the apoptotic kill rate. The apoptotic intensity function was chosen so that cells in later S-phase would be more susceptible to a drug dose than those cells early in S-phase, representative of lethal DNA damage near the late S-phase checkpoint (Kastan and Skapek, 2001).

Finally, the three age zero boundary conditions, which account for phase transition or division, are given by:

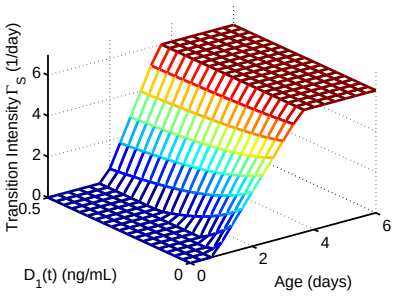

Fig. 2. Representation of the S-phase transition rate as a function of transition inhibiting drug concentration, $D_1(t)$, and age a.

$$N_G(0,t) = \int_0^\infty 2\Gamma_M(a)N_M(a,t)da \quad (11)$$

$$N_S(0,t) = \int_0^\infty \Gamma_G(a)N_G(a,t)da \quad (12)$$

$$N_M(0,t) = \int_0^\infty \Gamma_S(a,D_1(t))N_S(a,t)da \quad (13)$$

A summary of the parameters used for simulations can be found in Table 1. The parameters in the present study were selected to characterize a tumor with an approximate doubling time of 9 days, representative of Ht29 (a human colon carcinoma xenograft) tumor growth (Derenzini *et al.*, 2000).

4. CELL-CYCLE PBE SIMULATION

The cell-cycle PBE constructed above cannot be solved analytically; however, a plethora of numerical methods for solving problems of this class can be found in the literature. Solution techniques include finite difference (Mantzaris *et al.*, 2001), method of weighted residuals (Rice and Do, 1995; Ramkrishna, 2000; Mantzaris *et al.*, 2001) and finite element techniques (Mantzaris *et al.*, 2001). For the present problem, orthogonal collocation over finite elements was employed (Rice and Do, 1995). This approach divides the range of interest into a set of element subdomains. Orthogonal collocation, a method of weighted residuals solution technique, is then applied over each element. This method, which combines both method of weighted residual and finite element techniques, should outperform finite difference solutions in terms of accuracy as information from all collocation points within an element contribute to derivative calculations. Furthermore, orthogonal collocation on finite elements allows for the tailored arrangement of elements within the discretized domain such that more elements can be included in areas where transition, division, or apoptotic intensity functions may display extreme alterations in function value (Rice and Do, 1995).

Table 1. Model, transition function, division, and apoptosis function parameters.

Parameter	Value	Parameter	Value
a_{c_G}	3.75 day	β_G	4 $\frac{1}{\text{day}}$
a_{c_S}	2.4 day	β_S	6 $\frac{1}{\text{day}}$
a_{c_M}	1.5 day	β_M	6 $\frac{1}{\text{day}}$
k_{D0}	0.75 $\frac{1}{\text{day}}$	m_G	1.6
k_{D1}	1.5 $\frac{1}{\text{day}}$	m_S	5
k_{E0}	0.5 $\frac{1}{\text{day}}$	m_M	2.4
k_{E1}	0.75 $\frac{1}{\text{day}}$	m_D	0.15 $\frac{\text{ng}}{\text{mL}}$
k_A	4 $\frac{1}{\text{day}}$	K_M	2

Applying the method of weighted residuals reduces the cell-cycle PBE into a coupled set of ODEs:

$$\frac{d}{dt}\mathbf{N_G} = -(\mathbf{A_G} + \boldsymbol{\Gamma_G})\mathbf{N_G} - \mathbf{A_{G0}}N_{G0} \quad (14)$$

$$\frac{d}{dt}\mathbf{N_S} = -(\mathbf{A_S} + \boldsymbol{\Gamma_S} + \boldsymbol{\Gamma_E})\mathbf{N_S} - \mathbf{A_{S0}}N_{S0} \quad (15)$$

$$\frac{d}{dt}\mathbf{N_M} = -(\mathbf{A_M} + \boldsymbol{\Gamma_M})\mathbf{N_M} - \mathbf{A_{M0}}N_{M0} \quad (16)$$

In summary, each cell phase age domain was discretized into a set of elements. Each element was then divided into a number of internal collocation points with two additional collocation points corresponding to the element boundaries for a total of P, Q, and R collocation points within phases G, S, and M, respectively. Collocation point location within each cell phase was represented by a_{Gp}, a_{Sq}, and a_{Mr} with the cell phase density at each collocation point equal to N_{Gp}, N_{Sq}, and N_{Mr}. Next, the partial derivative of each cell phase population with respect to age was calculated as a linear combination from all the collocation points within an element at each collocation point within the system. The corresponding first derivative weight matrices are given by $\mathbf{A_G}$, $\mathbf{A_S}$, and $\mathbf{A_M}$ while $\boldsymbol{\Gamma_G}$ and $\boldsymbol{\Gamma_M}$ represent diagonal matrices with values $\boldsymbol{\Gamma}_G(\boldsymbol{p},\boldsymbol{p}) = \Gamma_G(a_{Gp})$ and $\boldsymbol{\Gamma}_M(\boldsymbol{r},\boldsymbol{r}) = \Gamma_M(a_{Mr})$, respectively. Similarly, $\boldsymbol{\Gamma_S}$ and $\boldsymbol{\Gamma_E}$ are defined as $\boldsymbol{\Gamma}_S(\boldsymbol{q},\boldsymbol{q}) = \Gamma_S(a_{Sq},D_1(t))$ and $\boldsymbol{\Gamma}_E(\boldsymbol{q},\boldsymbol{q}) = \Gamma_E(a_{Sq},E_1(t))$, respectively. These coupled ODEs apply to all collocation points within each phase excluding the age zero populations, N_{G0}, N_{S0}, and N_{M0}. Following age discretization, the cell density within each cell phase at age zero is given by the following algebraic relationships:

$$N_{G0}(t) = \sum_{r=1}^{R} 2w_{Mr}\Gamma_M(r,r)N_{Mr} \quad (17)$$

$$N_{S0}(t) = \sum_{p=1}^{P} w_{Gp}\Gamma_G(p,p)N_{Gp} \quad (18)$$

$$N_{M0}(t) = \sum_{q=1}^{Q} w_{Sq}\Gamma_S(q,q)N_{Sq} \quad (19)$$

Here, the previous integral boundary conditions (Equations (11), (12), and (13)) have been approximated by Gaussian quadrature (Rice and Do, 1995). Quadrature weights for the summations are given by w_{Gp}, w_{Sq}, and w_{Mr}. The eliminating and delaying drug equations remain unchanged (Equations (4)- (7)).

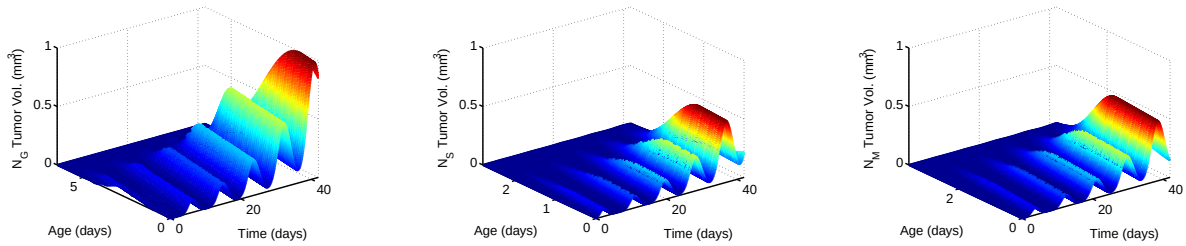

Fig. 3. Cell distribution within G-phase (left), S-phase (center), and M-phase (right) in the absence of treatment.

5. SIMULATION RESULTS

Model simulations were performed in MATLAB (©, 2004, The Mathworks, Natick, MA) using the function *dae4o.m* (Roberts, 2000).

Each of the three phases was separated into 18 elements with 2 internal collocation points apiece, amounting to 58 collocation points per phase. Approximately half of the elements are contained within the transition function region, $(a_{c_i} - 0.05)$ to $m_i a_{c_i}$, with two elements for all ages beyond. The rest of the elements are placed in the region between 0 and $(a_{c_i} - 0.05)$. Tighter element allocation begins prior to increases in transition intensity functions to ensure that any sharp increases in value will be captured.

The cell-cycle PBE was simulated for the test case of no drug delivery. Simulations were performed for 42 days with initial conditions:

$$N_G(a,0) = 0.08e^{\frac{-(a-0.27)^2}{0.16}} \tag{20}$$

$$N_S(a,0) = 0 \tag{21}$$

$$N_M(a,0) = 0 \tag{22}$$

Population distributions for each phase (G, S, and M) can be found in Figure 3. Starting at time zero with all cells located within G-phase, the progression of the population can be observed through each of the cell phases.

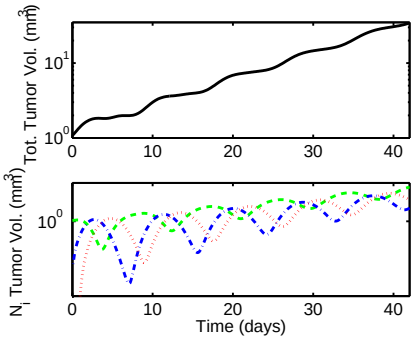

Fig. 4. Total population volume (top) and individual phase population volumes (bottom) for N_G (green, dashed), N_S (blue, dash-dot), and N_M (red, dotted) in mm^3.

Gradually, the distribution of cells spreads out over all three phases, eliminating the semi-discrete increases in population seen every 9 days in Figure 4 (top). While the overall tumor growth rate becomes nearly exponential by 35 days, oscillations continue to persist with respect to individual cell phase populations (Figure 4, bottom).

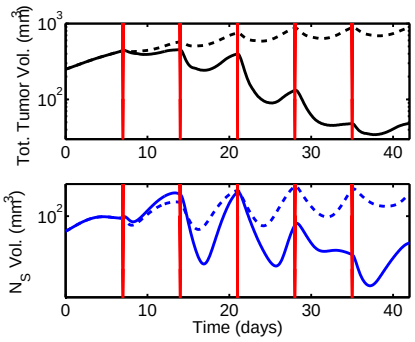

Fig. 5. Tumor progression versus time for total tumor volume (top) and S-phase volume (bottom). Apoptotic drug, E, was dosed every 7 days (vertical lines) starting at day 7 (dashed). Co-administration with transition inhibitor, D, (solid) is shown for comparison.

To evaluate the model response to drug effect, simulations were performed for two different dosing regimens. In the first case, doses of 10 mg of apoptotic drug were administered every seven days, starting on day 7, until day 35. The second case has co-administration of both drugs (10 mg of transition inhibiting and apoptosis inducing) on the same schedule. The simulation results are shown in Figure 5.

Final tumor volume predicted for the adjuvant treatment versus drug E alone was 48 vs. 894 mm^3, or a 19-fold reduction in final tumor volume. For comparison, simulations for untreated tumor growth or treatment with only drug D returned final tumor volumes of 7278 mm^3 and 5578 mm^3, respectively (not shown). The reduction in final volume for the adjuvant case partially resulted from drug D inhibiting progression rate into M-phase, thereby allowing for a greater susceptible total S-phase population. Consequently, cells remained in S-phase for increased periods of time, and as the tumor-kill term was formulated as a function of a cell age, the upper age portion of susceptible cells experienced a much greater apoptotic rate than would be achievable under normal phase progression.

6. SUMMARY

An age distributed cell-cycle population balance equation model was constructed to capture tumor growth. The assumed cycle transition and division intensity functions were capable of simulating near-exponential tumor growth (doubling time of 9 days) while maintaining information regarding population age within each individual cell phase. Models for growth inhibition and apoptotic effects for two theoretical drugs specific to the S-phase of the cell cycle were also developed and incorporated into the PBE. Simulations were able to reproduce typical drug-growth inhibitor interaction while retaining cell phase information following single-agent and co-delivery (Halicka *et al.*, 1997). Overall, the model produced stable results and was capable of tracking population progression through each phase. Additional experimental data are necessary to formulate biologically accurate transition, division, and apoptotic kernels for application to preclinical *in vivo* systems.

7. ACKNOWLEDGMENTS

The authors would like to acknowledge funding from a Whitaker Foundation Graduate Student Fellowship (JAF).

REFERENCES

Brown, J. M. and A. J. Giaccia (1998). The unique physiology of solid tumors: Opportunities (and problems) for cancer therapy. *Cancer Research* **58**, 1408–16.

Coleman, C. N. and J. B. Mitchell (2001). *Radiation Modifiers*. pp. 708–20. Cancer Chemotherapy and Biotherapy: Principles and Practice. 3rd ed.. Lippincott Williams and Wilkins.

Daoutidis, P. and M. A. Henson (2002). Dynamics and control of cell populations in continuous bioreactors. In: *Proceedings of CPC VI*. AIChE Symposia Series. CACHE Corporation.

Derenzini, M., D. Trere, A. Pession, M. Govoni, S. Valentina and P. Chieco (2000). Nucleolar size indicates the rapidity of cell proliferation in cancer tissues. *Journal of Pathology* **191**, 181–86.

Florian Jr., J. A., J. L. Eiseman and R. S. Parker (2003). Approximating cancer tumor growth dynamics using cell-cycle models in series. In: *AIChE Annual Meeting*. paper 439ab. San Francisco, CA.

Florian Jr., J. A., J. L. Eiseman and R. S. Parker (2004). A nonlinear model predictive control algorithm for breast cancer treatment. In: *DYCOPS*. Boston, Mass.

Fredrickson, A. G., D. Ramkrishna and H. M. Tsuchiya (1967). Statistics and dynamics of procaryotic cell populations. *Math. Biosci.* **1**, 327–74.

Halicka, H. D., K. Seiter, E. J. Feldman, F. Traganos, A. Mittelman, T. Ahmed and Z. Darzynkiewicz (1997). Cell cycle specificity of apoptosis during treatment of leukemias. *Apoptosis* **2**, 25–39.

Harrold, J. M., J. L. Eiseman, W. C. Zamboni and R. S. Parker (2003). A clinically relevant mixed integer approach to cancer chemotherapy treatment design. In: *AIChE Annual Meeting*. paper 478a. San Francisco, CA.

Kastan, Michael B. and Stephen X. Skapek (2001). *Molecular Biology of Cancer: The Cell Cycle*. Chap. 6, pp. 91–109. Cancer: principles & practice of oncology. Lippincott, Williams & Wilkins.

Mantzaris, N. V., F. Srienc and P. Daoutidis (2002). Nonlinear productivity control using a multi-staged cell population balance model. *Chem. Eng. Sci.* **57**, 1–14.

Mantzaris, N. V., P. Daoutidis and F. Srienc (2001). Numerical solution of multi-variable cell population balance models: I finite difference methods; II spectral methods; III finite element methods. *Comp. Chem. Eng.* **25**, 1411–81.

Martin, R. and K. L. Teo (1994). *Optimal Control of Drug Administration in Cancer Chemotherapy*. World Scientific. River Edge, NJ.

Morari, M. and E. Zafiriou (1989). *Robust Process Control*. Prentice-Hall, Englewood Cliffs, NJ.

Norton, L. (1988). A Gompertzian model of human breast cancer growth. *Cancer Res.* **48**, 7067–7071.

Panetta, J. C. and J. Adam (1995). A mathematical model of cycle–specific chemotherapy. *Math. Comput. Model.* **22**(2), 67–82.

Ramkrishna, D. (2000). *Population Balances: Theory and Applications to Particulate Systems in Engineering*. Academic Press. San Diego, CA.

Rice, R. G. and D. D. Do (1995). *Applied Mathematics and Modeling for Chemical Engineers*. Wiley. New York.

Roberts, Tony (2000). dae4o.m: A differential algebraic equation solver. MATLAB Central File Exchange.

The American Cancer Society (2004). Cancer facts & figures: 2004. URL: http://www.cancer.org/downloads/STT/CAFF_finalPWSecured.pdf.

Zamamiri, A. M., Y. Zhang, M. A. Henson and M. A. Hjortsø (2002). Dynamics analysis of an age distribution model of oscillating yeast cultures. *Chem. Eng. Sci.* **57**, 2169–2181.

Zhu, G.-Y., A. Zamamiri, M. A. Henson and M. A. Hjortsø (2000). Model predictive control of continuous yeast bioreactors using cell population balance models. *Chem. Eng. Sci.* **55**, 6155–6167.